Theoretical Analysis of Indirect and Direct Solar Regenerators for Liquid Desiccant Systems

Fernando M. Gómez-Castro and Ursula Eicker

University of Applied Sciences Stuttgart/Centre of Applied Research Sustainable Energy Technologies zafh.net, Stuttgart (Germany)

Abstract

Solar liquid desiccant air-conditioning systems have recently attracted attention due to their sustainability and good energy saving potential, since only heat is required in the solution regeneration process. The solar regenerators can be classified as indirect and direct regeneration units. In the first type, the solar heat can be transferred either to the air stream via solar air collectors or a combination of solar water collectors and water-to-air heat exchangers or to the liquid desiccant via a combination of solar water collectors and water-to-solution heat exchangers before entering the regeneration chamber. In the second type, the diluted solution is exposed simultaneously to the solar radiation and the air stream within a solar collector/regenerator. A performance comparison between both types of regeneration units is presented in this paper. The simulation results demonstrate that direct solar regenerators have a high potential for enhancing the water desorption rate from a diluted solution and, consequently, the air dehumidification capacity within the absorber.

Keywords: Liquid desiccant, indirect solar regenerator, solar collector/regenerator, performance comparison.

1. Introduction

Air conditioning in buildings is a large and growing market, almost exclusively covered with electrical compression systems. Therefore, in order to supply this market with sustainable technologies, cost-effective solar thermally-driven liquid sorption systems, which rely on the capacity of hygroscopic solutions in removing the air moisture content by the absorption process (Grossman and Johannsen, 1981) and on the solar heat for regenerating the solution in a temperature range of 40 to 70 °C (Katejanekarn and Kumar, 2008), need to be developed.

Indirect solar regenerated systems comprise the main components absorber, in which the moisture of the inlet process air is removed by bringing it into contact with sprinkled desiccant solution, and regenerator, in which the water content of the solution gradually diluted within the absorber is reduced by enhancing both its temperature and vapour pressure, and by subsequently removing the evaporated water through an air stream. Among the direct contact sorption chambers commonly used as heat and mass exchangers in both the air dehumidification and solution regeneration processes stand out the packed bed towers, which are filled with random or structured packing materials that increase the mass transfer area per unit volume as well as the contact time between the fluids involved in the sorption process, leading to more compact units (Martin and Goswami, 2000). Nevertheless, they require high enough solution mass flow rates for a proper wetting of the packing material as well as high fan energy consumption due to high air pressure drops. The heat required for the regeneration process can be supplied by either air-led (Kabeel et al., 2017) or water-based solar collectors (Jamar et al., 2016) and, more recently, by photovoltaic/thermal (PV/T) modules (Guo et al. 2017), which provide both heat for reconcentrating the liquid desiccant and electricity for powering the parasitic components (fans and pumps). The resulting strong solution is then stored without thermal losses for carrying out the air dehumidification process when solar radiation is not available. The dehumidified process air, heated by exothermic reactions during the moisture absorption in the desiccant solution, is generally precooled by the outdoor air or the return air from the room and moistened adiabatically in the next step to produce the desired cooling effect for air conditioning applications. However, some barriers like the high costs of manufacture and installation of the equipment, high system complexity due to the large number of individual components and the need of highly sophisticated control systems drastically limit the market entrance of indirect solar regenerated

doi:10.18086/swc.2017.28.09 Available at http://proceedings.ises.org

liquid desiccant systems (Gommed and Grossman, 2007).

The needed system simplification and its associated cost reduction can be accomplished by transferring the regeneration process into the solar collector. In this way, and contrary to the indirect solar regenerator, the hygroscopic solution is exposed simultaneously to the solar radiation and the air stream, which contributes to enhance the thermal regeneration efficiency. The direct solar regenerators can be classified as open-type, closed-type and convective-type. Several theoretical works (Yang and Wang, 2001; Kaushik et al., 1992) and experimental studies (Gezahegn et al., 2013; Kabeel, 2005; Hawlader et al., 1997) carried out under different operating conditions have demonstrated that the glazed forced convective collector/regenerator performs generally better than the other types in both humid and temperate climates, since its glazing limits the thermal losses to the ambient and also keeps the desiccant solution free from contamination due to dirt and rains.

However, there is a lack of works in the literature on the performance comparison between the indirect solar regeneration chambers and the solar collector/regenerators. This paper provides some light on this issue by comparing the performance curves obtained for both types of solar regenerators at specified operating conditions from calculation models developed in the equation-oriented simulation environment EES and by outlining under what conditions the direct solar regenerator outperforms the indirect ones.

2. System description

Three indirect solar regeneration units, which essentially comprise an adiabatic packed bed sorption reactor, an array of solar water/air heaters as well as heat exchangers, and a forced convective direct solar regenerator were theoretically analysed in this study. These configurations are depicted in Fig. 1 and described as follows:

- **Variant SWH+WA-HX+Reg (solar water heater + water-air heat exchanger for preheating of the regenerating air):** A 16 m² south-oriented collector field of solar water heaters (Topson TX) with 40% aqueous propylene glycol solution as working fluid and a tilt angle of 30° is connected with a finned coil water-air heat exchanger (WA-HX, Brazetek BT-HTL 12×12), in which the regenerating air stream is warmed-up before entering a counterflow adiabatic regeneration chamber (see Fig. 1(a)), whose packed bed (400 mm width × 400 mm length × 400 mm height) is filled with ceramic Novalox® saddles (volumetric mass transfer area = 255 m²/m³, void fraction = 0.74).
- **Variant SAH+Reg:** A similar field of compact solar air heaters (SAH TwinSolar) is directly coupled to the aforementioned packed bed regenerator as shown in Fig. 1(b).
- **Variant SWH+WS-HX+Reg:** The finned coil water-air heat exchanger of the variant SWH+WA-HX+Reg is replaced by a water-solution parallel plates heat exchanger (WS-HX, Kaori K095) for heating up the liquid sorbent before its entrance to the sorption reactor (see Fig. 1(c)).
- **Variant SWH+WS-HX+WA-HX+Reg:** A finned coil water-air heat exchanger and a water-solution parallel plates heat exchanger, identical to those of the variants SWH+WA-HX+Reg and SWH+WS-HX+Reg respectively, are connected in parallel with the solar water heaters field for simultaneously preheating the regenerating air and the desiccant solution (see Fig. 1(d)).
- **Variant SCR:** The diluted hygroscopic liquid and the regenerating air stream are simultaneously, directly heated through a field of counterflow, single-glazed solar collector/regenerators for reconcentrating the desiccant solution (see Fig. 1(e)).

Based on the energy conservation laws, thermodynamic equilibrium, as well as the heat and mass transfer laws for each system component, all these regenerator variants were modelled in the equation-oriented simulation environment EES to assess the water desorption rate ($\Delta \dot{m}_{des}$) for the specified operating conditions, which indicates the change of the amount of water vapour transferred to the air stream $\dot{m}_a$ and, therefore, evaporated from the hygroscopic solution per unit time:

$$\Delta \dot{m}_{des} = \dot{m}_a \cdot (\chi_{a,out} - \chi_{a,in}) \quad \text{(eq. 1)}$$

Where $\chi_{a,in}$ and $\chi_{a,out}$ are the absolute humidities of the air at the inlet and outlet of a sorption unit, respectively.

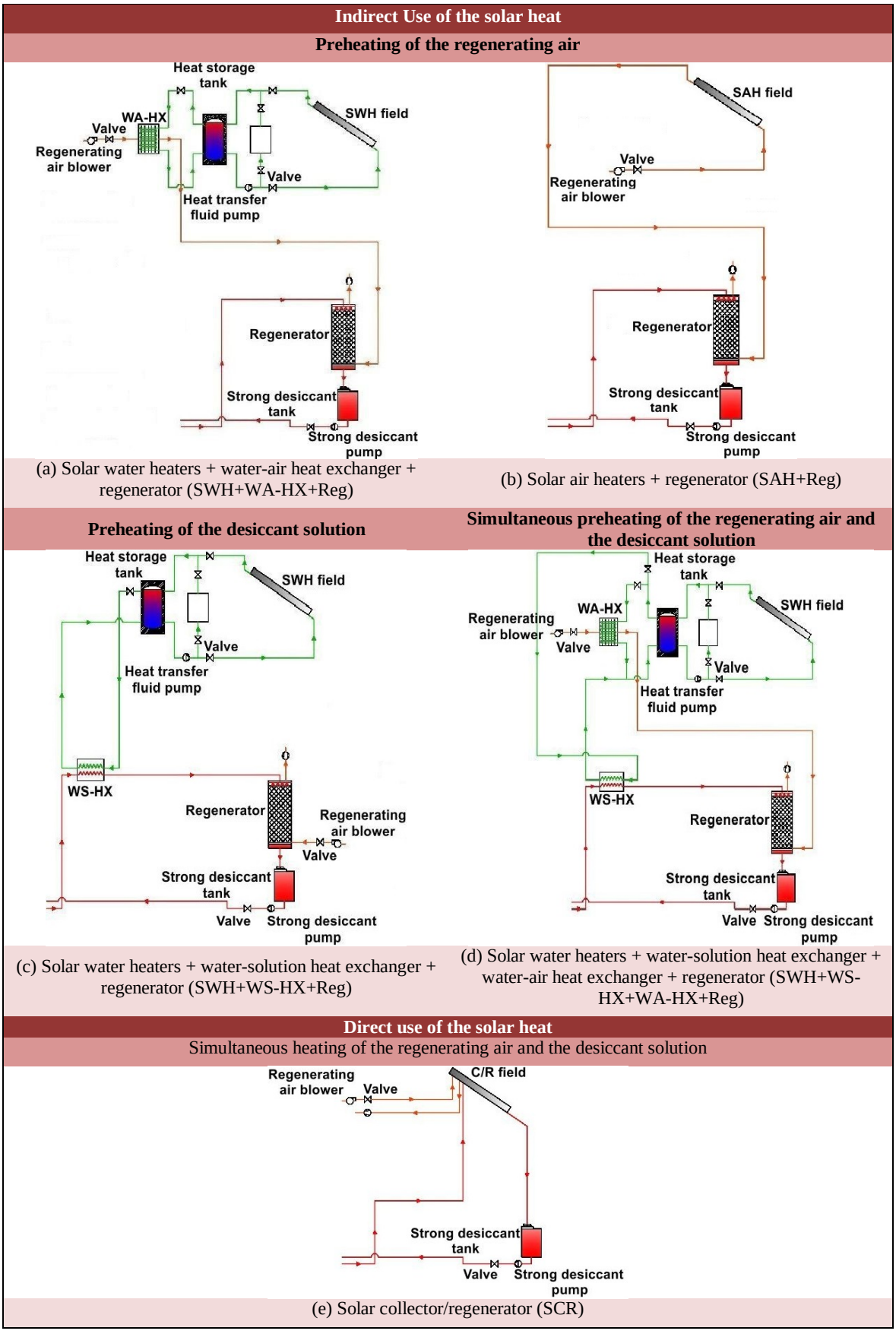

(a) Solar water heaters + water-air heat exchanger + regenerator (SWH+WA-HX+Reg)

(b) Solar air heaters + regenerator (SAH+Reg)

(c) Solar water heaters + water-solution heat exchanger + regenerator (SWH+WS-HX+Reg)

(d) Solar water heaters + water-solution heat exchanger + water-air heat exchanger + regenerator (SWH+WS-HX+WA-HX+Reg)

(e) Solar collector/regenerator (SCR)

Fig. 1: Analysed variants of the solar regenerators with indirect and direct (pre)heating of the regenerating air and the desiccant solution.

3. Mathematical modeling of the system components

3.1 Indirect solar regenerators

The efficiency of the sola collector η_c is given in terms of the average bulk temperature of the heat transfer medium $T_{f,m}$ and the ambient temperature T_{amb} by:

$$\eta_c=\eta_0-U_{L,1}\cdot\left[\left(T_{f,m}-T_{amb}\right)/G_{g,c}\right]-U_{L,2}\cdot G_{g,c}\cdot\left[\left(T_{f,m}-T_{amb}\right)/G_{g,c}\right]^2 \quad \text{(eq. 2)}$$

Where η_0, $U_{L,1}$, and $U_{L,2}$ are the collector optical efficiency, the linear heat loss coefficient and the quadratic heat loss coefficient for the solar collectors. For the collectors employed in this simulation, these coefficients are summarized in Tab. 1.

Tab. 1: Model parameters for the analysed air- and water-based solar collectors.

Parameter	TwinSolar compact	Topson TX
η_0 [-]	0.82	0.797
$U_{L,1}$ [W/(m² K)]	6.50	2.833
$U_{L,2}$ [W/(m² K²)]	0.032	0.0133

Fig. 2 shows a schematic diagram of the finite difference of a conventional counterflow regeneration unit with the heat and mass transfer interactions between the liquid desiccant and the regenerating air stream. By assuming negligible heat loss from or gain to the finite element, the 1D steady-state mass and energy balances can be written as follows:

Desiccant solution:

Mass balance

$$\dot{m}_{s,i}\cdot\xi_{s,i}=\dot{m}_{s,i-1}\cdot\xi_{s,i-1} \quad \text{(eq. 3)}$$

$$\dot{m}_{s,i}=\dot{m}_{s,i-1}-\Delta\dot{m}_{des,m,i} \quad \text{(eq. 4)}$$

Energy balance

$$\dot{m}_{s,i-1}\cdot h_{s,i-1}=\dot{m}_{s,i}\cdot h_{s,i}+h_{conv,s\text{-}a,m,i}\cdot A_{w,i}\cdot\left(T_{s,m,i}-T_{a,m,i}\right)+\Delta\dot{m}_{des,m,i}\cdot\left(h_{fg,i}+\Delta h_{d,i}\right) \quad \text{(eq. 5)}$$

Regenerating air:

Mass balance

$$\dot{m}_a\cdot\chi_{a,i-1}=\dot{m}_a\cdot\chi_{a,i}+\Delta\dot{m}_{des,m,i} \quad \text{(eq. 6)}$$

Energy balance

$$\dot{m}_a\cdot h_{a,i}+h_{conv,s\text{-}a,m,i}\cdot A_{w,i}\cdot\left(T_{s,m,i}-T_{a,m,i}\right)+\Delta\dot{m}_{des,m,i}\cdot\left(h_{fg,i}+\Delta h_{d,i}\right)=\dot{m}_a\cdot h_{a,i-1} \quad \text{(eq. 7)}$$

Where $\dot{m}$, h and T stand for the mass flow rate [kg/s], the specific enthalpy [J/kg] and the temperature [K] of the fluids involved in the regeneration process, while χ_a and ξ_s are the absolute humidity of the air [kg/kg] and the mass fraction of the hygroscopic liquid. The subscripts a and s stand for the air and the desiccant solution, whereas the subscripts i-1 and i denote the inlet/outlet and outlet/inlet characteristics of the solution/air. The symbols $h_{conv,s\text{-}a,m,i}$, $A_{w,i}$, $\Delta\dot{m}_{des,m,i}$, $h_{fg,i}$ and $\Delta h_{d,i}$ correspond to the local values of the convective heat transfer coefficient between the solution film and the air stream [W/(m² K)], the finite element area wetted by the

solution [m²], the water desorption rate [kg/s], the latent heat of water vaporisation [J/kg] and the differential enthalpy of dilution [J/kg], respectively.

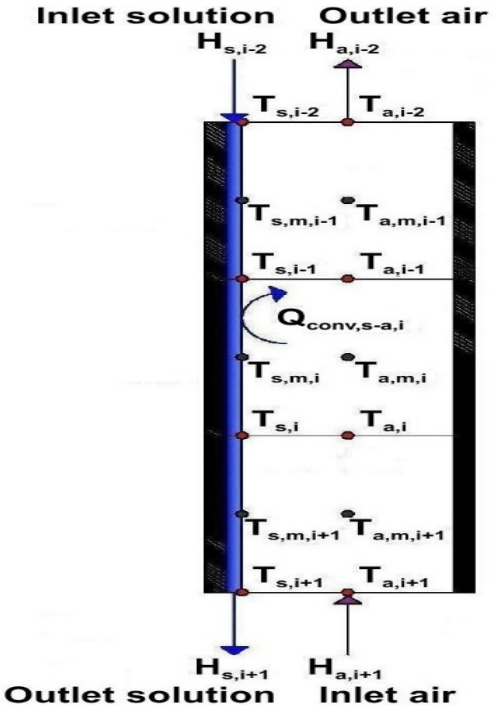

Fig. 2: Heat and mass transfer mechanisms in a finite element of the adiabatic counterflow packed bed regenerator.

On the other hand, the local water desorption rate $\Delta\dot{m}_{des,m,i}$ from the diluted liquid sorbent can be calculated as follows:

$$\Delta\dot{m}_{des,m,i}=\frac{\beta_{m,i}\cdot M_{H_2O}}{R_m\cdot T_{a,m,i}}\cdot A_{w,i}\cdot\left(p_{s,m,i}-p_{a,m,i}\right) \qquad \text{(eq. 8)}$$

With M_{H_2O} and R_m as the molar mass of the water vapour (0.01802 kg/mol) and the molar gas constant (8.31451 J/(mol K)), and $p_{s,m,i}$ and $p_{a,m,i}$ as the vapour pressures [Pa] of the solution and the regenerating air at their average temperatures $T_{s,m,i}$ and $T_{a,m,i}$.

The local mass transfer coefficient based on the gas-phase concentration $\beta_{m,i}$ [m/s] is determined in terms of the heat transfer coefficient $h_{conv,s-a,m,i}$ by applying the Chilton-Colburn analogy:

$$\beta_{m,i}=\frac{h_{conv,s-a,m,i}}{\rho_{a,m,i}\cdot c_{p,a,m,i}\cdot Le_a^{2/3}} \qquad \text{(eq. 9)}$$

Where $\rho_{a,m,i}$, $c_{p,a,m,i}$ and Le_a stand for the density [kg/m³], the isobaric specific heat capacity [J/(kg K)] of the regenerating air, and the Lewis number of the water vapour-air mixture. The local convective heat transfer coefficient between a fluid and the particles in the packed bed reactor is calculated according to the relationships given in the VDI Heat Atlas (Gnielinski, 2010).

3.2 Direct solar regenerators

The simultaneous heat and mass transfer mechanisms occurring within a single-glazed forced convective collector/regenerator are shown in Fig. 3. By neglecting the gradients of temperature and water content in both the air stream and the liquid film along the collector width, disregarding the heat conduction and mass diffusion

in both the air and the solution along their flow directions, and considering uniform wall temperature and concentration boundary conditions for the heat and mass transfer in the finite element, the following 1D steady-state mass and energy balances can be formulated for the counterflow case:

Collector housing;

Energy balance

$$U_{cond,p\text{-}h,m,i}\cdot\left(T_{p,m,i}-T_{h,m,i}\right)=h_{conv,h\text{-}amb,m,i}\cdot A_{c,i}\cdot\left(T_{h,m,i}-T_{amb}\right) \quad \text{(eq. 10)}$$
$$+h_{rad,h\text{-}sky,m,i}\cdot A_{c,i}\cdot\left(T_{h,m,i}-T_{sky}\right)$$
$$+h_{rad,h\text{-}gr,m,i}\cdot A_{c,i}\cdot\left(T_{h,m,i}-T_{gr}\right)$$

Absorber plate:

Energy balance

$$\left[\left(\tau_g\cdot\tau_s\cdot\alpha_p\right)_{eff}\cdot F_w+\left(\tau_g\cdot\alpha_p\right)_{eff}\cdot(1-F_w)\right]\cdot G_{g,c}\cdot A_{c,i}=U_{cond,p\text{-}h,m,i}\cdot A_{c,i}\cdot\left(T_{p,m,i}-T_{h,m,i}\right) \quad \text{(eq.11)}$$
$$+h_{conv,p\text{-}a,m,i}\cdot(1-F_w)\cdot A_{c,i}\cdot\left(T_{p,m,i}-T_{a,m,i}\right)$$
$$+h_{conv,p\text{-}s,m,i}\cdot F_w\cdot A_{c,i}\cdot\left(T_{p,m,i}-T_{s,m,i}\right)$$
$$+h_{rad,p\text{-}g,m,i}\cdot(1-F_w)\cdot A_{c,i}\cdot\left(T_{p,m,i}-T_{g,m,i}\right)$$

Desiccant solution:

Mass balance (see eq. 3 and eq. 4)

Energy balance

$$\dot{m}_{s,i-1}\cdot h_{s,i-1}+h_{conv,p\text{-}s,m.i}\cdot F_w\cdot A_{c,i}\cdot\left(T_{p,m,i}-T_{s,m,i}\right)=\dot{m}_{s,i}\cdot h_{s,i}+\Delta\dot{m}_{des,m,i}\cdot\left(h_{fg,i}+\Delta h_{d,i}\right) \quad \text{(eq.12)}$$
$$+h_{conv,s\text{-}a,m,i}\cdot F_w\cdot A_{c,i}\cdot\left(T_{s,m,i}-T_{a,m,i}\right)$$
$$+h_{rad,s\text{-}g,m,i}\cdot F_w\cdot A_{c,i}\cdot\left(T_{s,m.i}-T_{g,m,i}\right)$$

Regenerating air:

Mass balance (see eq. 6)

Energy balance

$$\dot{m}_a\cdot h_{a,i}+\Delta\dot{m}_{des,m,i}\cdot\left(h_{fg,i}+\Delta h_{d,i}\right)+h_{conv,s\text{-}a,m,i}\cdot F_w\cdot A_{c,i}\cdot\left(T_{s,m,i}-T_{a,m,i}\right) \quad \text{(eq.13)}$$
$$+h_{conv,p\text{-}a,m,i}\cdot(1-F_w)\cdot A_{c,i}\cdot\left(T_{p,m,i}-T_{a,m,i}\right)+h_{conv,g\text{-}a,m,i}\cdot A_{c,i}\cdot\left(T_{g,m,i}-T_{a,m,i}\right)=\dot{m}_a\cdot h_{a,i-1}$$

Glass cover:

Energy balance

$$\alpha_g\cdot G_{g,c}\cdot A_{c,i}+h_{rad,s\text{-}g,m,i}\cdot F_w\cdot A_{c,i}\cdot\left(T_{s,m,i}-T_{g,m,i}\right)+h_{rad,p\text{-}g,m,i}\cdot\left(1-F_w\right)\cdot A_{c,i}\cdot\left(T_{p,m,i}-T_{g,m,i}\right)= \quad \text{(eq.14)}$$
$$h_{conv,g\text{-}a,m,i}\cdot A_{c,i}\cdot\left(T_{g,m,i}-T_{a,m,i}\right)+U_{conv,g\text{-}amb,m.i}\cdot A_{c,i}\cdot\left(T_{g,m,i}-T_{amb}\right)$$
$$+U_{rad,g\text{-}sky,m,i}\cdot A_{c,i}\cdot\left(T_{g,m,i}-T_{sky}\right)+U_{rad,g\text{-}gr,m,i}\cdot A_{c,i}\cdot\left(T_{g,m,i}-T_{gr}\right)$$

With $\dot{m}$, h and T as the mass flow rate [kg/s], the specific enthalpy [J/kg] and the temperature [K] of the fluids involved in the regeneration process. The subscripts *h*, *p*, *s*, *a*, *g*, *amb*, *sky* and *gr* refer to the collector housing, the absorber plate, the hygroscopic solution, the regenerating air, the glass cover, the ambient, the sky and the ground, while the subscripts *i-1* and *i* indicate the inlet/outlet and outlet/inlet conditions of the solution/air. The symbols F_w, $A_{c,i}$, $\Delta\dot{m}_{des,m,i}$, $h_{fg,i}$ and $\Delta h_{d,i}$ correspondingly stand for the wetting factor, the total finite element

area [m²] as well as the local values of the water desorption rate [kg/s], the latent heat of water vaporisation [J/kg] and the differential enthalpy of dilution [J/kg]. The approaches to estimate the effective transmittance-absorptance products for the glass cover-absorber plate $\left(\tau_g \cdot \alpha_p\right)_{eff}$ and the glass cover-desiccant solution-absorber plate $\left(\tau_g \cdot \tau_s \cdot \alpha_p\right)_{eff}$ optical systems are given by Duffie and Beckman (2013). Finally, h_{conv}- U_{conv}, h_{rad} - U_{rad}, and U_{cond} denote the convective heat transfer coefficients, the radiative heat transfer coefficients, and the heat conductance value, respectively.

The air channel of a forced convective collector/regenerator is asymmetrically heated since its absorber plate is considerably warmer than its glass cover. For analysis purposes, the convective heat transfer coefficients between the absorber plate and the air stream ($h_{conv,p\text{-}a,m,i}$), the desiccant solution and the air stream ($h_{conv,s\text{-}a,m,i}$), and the glazing and the air stream ($h_{conv,g\text{-}a,m,i}$) are considered to be equal. In this way, the convective heat transfer coefficient $h_{conv,s\text{-}a,m,i}$ [W/(m² K)] is evaluated as follows:

$$h_{conv,s\text{-}a,m,i} = Nu_{s\text{-}a} \cdot k_{a,m,i} / D_h \qquad \text{(eq. 15)}$$

For laminar flow ($Re_{a,D_h} \leq 2300$), the Nusselt number $Nu_{s\text{-}a,lam}$ can be determined by means of the correlation of Mercer et al. (1967) for one-sided heated air channels at constant wall temperature:

$$Nu_{s\text{-}a,lam} = 4.86 + \frac{0.0606 \cdot \left(Re_{a,D_h} \cdot Pr_a \cdot D_h / L_c\right)^{1.2}}{1 + 0.0909 \cdot \left(Re_{a,D_h} \cdot Pr_a \cdot D_h / L_c\right)^{0.7} \cdot Pr_a^{0.17}} \qquad \text{(eq. 16)}$$

For turbulent flow ($Re_{a,D_h} \geq 3000$), in which the influences of the boundary conditions and the channel geometry are minor, the modified equation of Petukhov (Gnielinski, 1976) is used for assessing the Nusselt number $Nu_{s\text{-}a,turb}$:

$$Nu_{s\text{-}a,turb} = \left[\frac{(f/8) \cdot Re_{a,D_h} \cdot Pr_a}{1 + 12.7 \cdot \sqrt{f/8} \cdot \left(Pr_a^{2/3} - 1\right)}\right] \cdot \left[1 + \left(\frac{D_h}{L_c}\right)^{2/3}\right] \qquad \text{(eq. 17)}$$

$$f = \left\{0.78 \cdot Ln\left(Re_{a,D_h}\right) - 1.5\right\}^{-2}$$

With L_c and D_h as the channel length [m] and the hydraulic diameter [m].

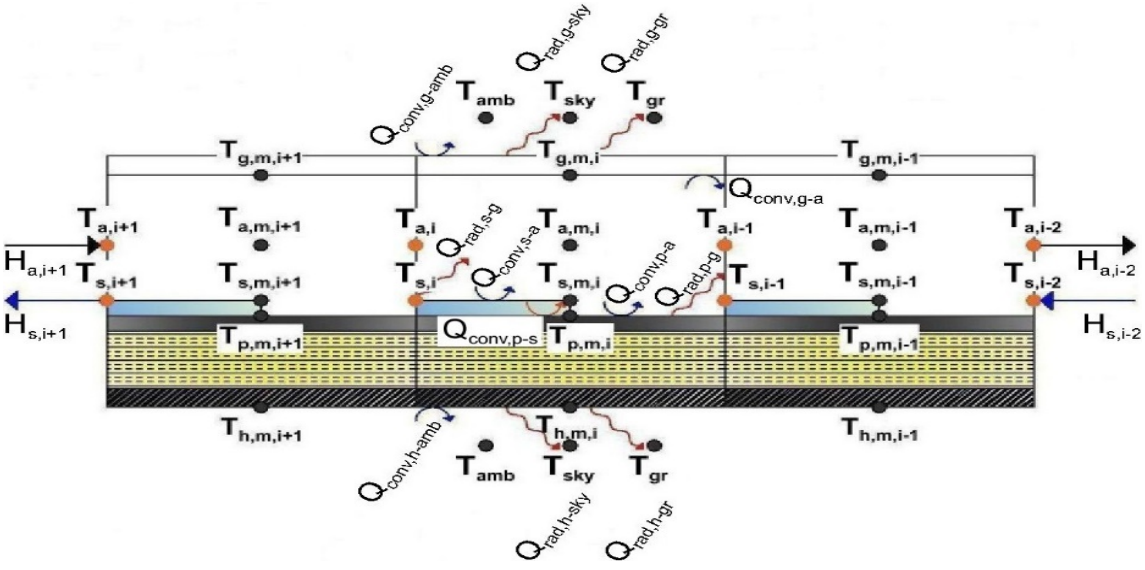

Fig. 3: Heat and mass transfer mechanisms in a finite element of the counterflow collector/regenerator.

4. Simulation results and discussion

This section presents the performance comparisons between the indirect and direct solar thermal regeneration units. Aqueous lithium chloride solution (LiCl-H_2O) was used as liquid desiccant. The parameters for this simulation study are summarised in Tab. 2.

Tab. 2: Parameters for the simulation of the analysed solar regeneration systems.

Component	Operating parameter	Unit	Range (reference value)	Variant
Solar water heater	Solar radiation	W/m²	800	SWH+WA-HX+Reg, SWH+WS-HX+Reg, SWH+WS-HX+WA-HX+Reg
	Collector area	m²	16	
	Tilt angle	°	30	
	Fluid volumetric flow rate	l/h	240	
	Fluid mass fraction	%	40	
	Inlet fluid temperature	°C	40	
WA-HX	Fluid volumetric flow rate	l/h	240	SWH+WA-HX+Reg
			120	SWH+WS-HX+WA-HX+Reg
	Air volumetric flow rate	m³/h	100-400 (300)	SWH+WA-HX+Reg, SWH+WS-HX+WA-HX+Reg
	Inlet air temperature	°C	24-40 (30)	
	Inlet air absolute humidity	g/kg	10.6-18.8 (10.6)	
WS-HX	Fluid volumetric flow rate	l/h	240	SWH+WS-HX+Reg
			120	SWH+WS-HX+WA-HX+Reg
	Solution volumetric flow rate	l/h	100-400 (200)	SWH+WS-HX+Reg, SWH+WS-HX+WA-HX+Reg
	Inlet solution temperature	°C	40-70 (50)	
	Inlet solution mass fraction	%	34-42 (37)	
Solar air heater	Air volumetric flow rate	m³/h	100-400 (300)	SAH+Reg
	Inlet air temperature	°C	24-40 (30)	
	Inlet air absolute humidity	g/kg	10.6-18.8 (10.6)	
Regenerator	Air volumetric flow rate	m³/h	100-400 (300)	SWH+WA-HX+Reg, SAH+Reg, SWH+WS-HX+Reg, SWH+WS-HX+WA-HX+Reg
	Inlet air temperature	°C	24-40 (30)	SWH+WS-HX+Reg
	Inlet air absolute humidity	g/kg	10.6-18.8 (10.6)	SWH+WA-HX+Reg, SAH+Reg, SWH+WS-HX+Reg, SWH+WS-HX+WA-HX+Reg
	Solution volumetric flow rate	l/h	100-400 (200)	
	Inlet solution temperature	°C	40-70 (50)	SWH+WA-HX+Reg, SAH+Reg
	Inlet solution mass fraction	%	34-42 (37)	SWH+WA-HX+Reg, SAH+Reg, SWH+WS-HX+Reg, SWH+WS-HX+WA-HX+Reg
Collector/regenerator	Air volumetric flow rate	m³/h	100-400 (300)	SCR
	Inlet air temperature	°C	24-40 (30)	
	Inlet air absolute humidity	g/kg	10.6-18.8 (10.6)	
	Solution volumetric flow rate	l/h	100-400 (200)	
	Inlet solution temperature	°C	40-70 (50)	
	Inlet solution mass fraction	%	34-42 (37)	

4.1 Effects of inlet air parameters on the regeneration performance

Fig. 4 shows that, for all configurations, the desorption rate increased with the rise of the inlet air temperature due to the enhancement in the driving force for the heat transfer between the regenerating air and the hygroscopic solution, which consequently augmented the temperature and the vapour pressure of the liquid sorbent. The desorption rate obtained from the direct solar regenerator (SCR) was in average 11% and 9% greater than those respectively achieved from the variants with indirect solar preheating of both air and liquid sorbent (SWH+WS-HX+WA-HX+Reg) and of only desiccant solution (SWH+WS-HX+Reg), which were the best indirect solar regeneration units at the analysed operating conditions. By contrast, the regenerators with air preheating via solar air heaters (SAH+Reg) and solar water heaters (SWH+WA-HX+Reg) exhibited the worst performances among the conventional regeneration units with average desorption rates 37 % and 49% lower than that from the direct solar regenerator.

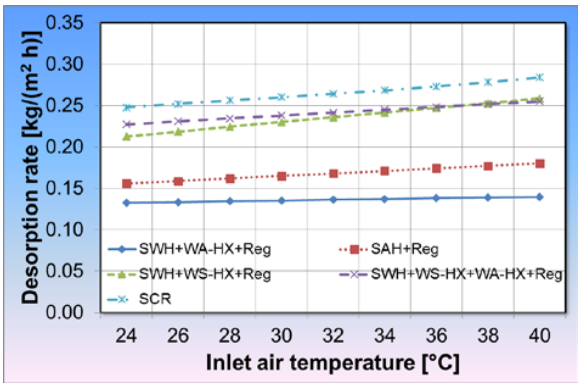

Fig. 4: Effect of the inlet air temperature on the desorption rate of the solar regenerators with indirect and direct (pre)heating of the regenerating air and the desiccant solution.

The desorption rate linearly decreased in all analysed solar regenerators with increasing absolute humidity of the air stream (see Fig. 5) due to the inherent rise in the air vapour pressure, which indeed diminished the vapour pressure difference between the desiccant solution and the air. This decrease was less severe in the direct solar regenerator than in the conventional regeneration units at the analysed operating conditions. The desorption rates achieved with the variants with simultaneous indirect solar preheating of the liquid sorbent and the air (SWH+WS-HX+WA-HX+Reg) and indirect solar preheating of the desiccant solution came next and were on average about 17% and 21% lower than those for direct solar regenerators, respectively. On the other hand, the regeneration systems with air preheating through solar air heaters (SAH+Reg) and solar water heaters (SWH+WA-HX+Reg) had the worst desorption rates, which were approximately 47% and 60% less than the respective value for collector/regenerators.

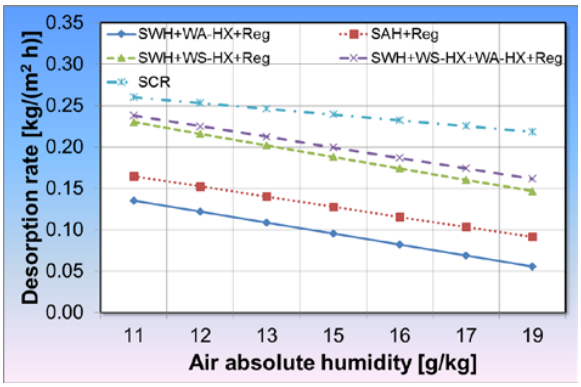

Fig. 5: Effect of the air absolute humidity on the desorption rate of the solar regenerators with indirect and direct (pre)heating of the regenerating air and the desiccant solution.

According to Fig. 6, the desorption rate for all configurations augmented at the analysed operating conditions by increasing the air volumetric flow rate due to the enhancement in the mass transfer coefficient, which counteracted the decrease in the solution temperature and its vapour pressure. From an air volumetric flow rate

of 300 m³/h ($\dot{m}_a/\dot{m}_{s,in}=1.187$ with $\dot{V}_{s,in}=200\ l/h$), the direct solar regenerator exhibited considerably high values of said performance index compared with those of indirect solar regenerators because of the proximity to the turbulent regime of air flow within the collector/regenerator channel ($Re_{a,ch}=2374$). In average, the desorption rate achieved with the direct solar regenerator was 14% greater than those for the variants with indirect solar preheating of air and liquid desiccant (SWH+WS-HX+WA-HX+Reg and SWH+WS-HX+Reg). Moreover, the variants with indirect solar preheating of air by means of solar air heaters (SAH+Reg) and solar water heaters (SWH+WA-HX+Reg) were clearly outperformed with average desorption rates 44% and 53% lower than that of the direct solar regenerator.

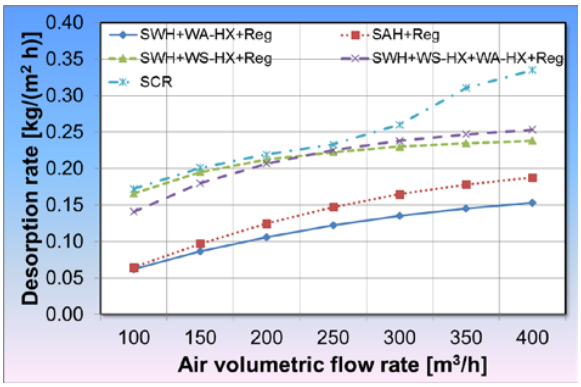

Fig. 6: Effect of the air volumetric flow rate on the desorption rate of the solar regenerators with indirect and direct (pre)heating of the regenerating air and the desiccant solution.

4.2 Effects of inlet solution parameters on the regeneration performance

When the desiccant solution entered the analysed regeneration units at high temperatures, the consequent increasing in the heat and mass transfer driven potentials led to higher desorption rates (see Fig. 7). Comparing with the effect of the inlet air temperature, it can be concluded that preheating the desiccant solution was more efficient than preheating the air stream. Although the average desorption rate attained with the direct solar regenerator was approximately 11%, 17%, 26% and 37% higher than those corresponding to the conventional regeneration units SWH+WS-HX+WA-HX+Reg, SWH+WS-HX+Reg, SAH+Reg and SWH+WA-HX+Reg, the performance differences among them were considerably reduced from an inlet solution temperature of 60°C.

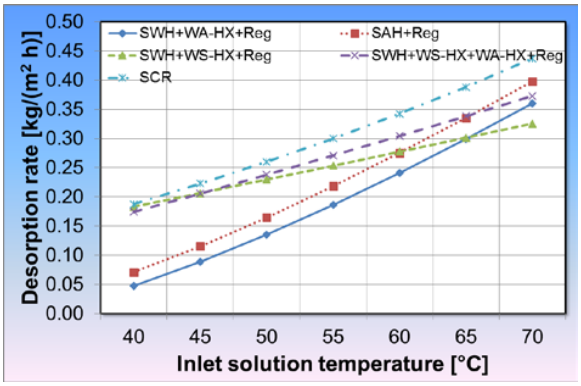

Fig. 7: Effect of the inlet solution temperature on the desorption rate of the solar regenerators with indirect and direct (pre)heating of the regenerating air and the desiccant solution.

Under the given operating conditions, the higher the solution mass fraction, the lower the desorption rate for all the analysed regeneration units due to the lower vapour pressure of the solution, which indeed reduced the mass transfer driven potential as shown in Fig. 8. The desorption rate achieved with the direct solar regenerator was 10% and 13% higher than the corresponding values for the variants with indirect solar preheating of both the air and desiccant solution (SWH+WS-HX+WA-HX+Reg) and of only liquid sorbent (SWH+WS-HX+Reg). Besides, the performance of the configurations with indirect solar preheating of air by using solar air heaters (SAH+Reg) and solar water heaters (SWH+WA-HX+Reg) were widely surpassed with average desorption rates 39% and 51% lower than that of the solar collector/regenerator.

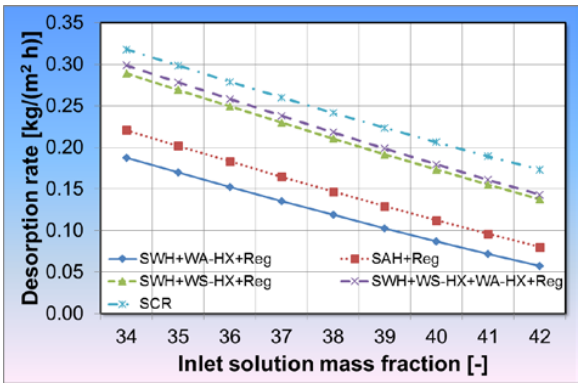

Fig. 8: Effect of the inlet solution mass fraction on the desorption rate of the solar regenerators with indirect and direct (pre)heating of the regenerating air and the desiccant solution.

For the analysed range of operating conditions, the increase of the solution volumetric flow rate affected in different ways the desorption rate for direct and indirect solar regenerators (see Fig. 9). In the case of the collector/regenerator, the desorption rate strongly decreased with the rise of the solution volumetric flow rate due to the reduced residence time of the liquid sorbent within said device, which contributed to diminish both the solar warming of the solution and the resulting mass transfer potential. On the other hand, the desorption rate obtained from the indirect solar regeneration units exhibited the inverse behaviour since the shortening of the residence time of solution within the sorption reactor led to the decrease of the temperature falls for both the air and the liquid sorbent, thus keeping the heat and mass transfer driven potentials relatively high. It was observed that the direct solar regenerator clearly outperformed the investigated indirect solar regeneration units until reaching a critical solution volumetric flow rate of approximately 225 l/h ($\dot{m}_a/\dot{m}_{s,in}=1.282$ with $\dot{V}_a=300\ m^3/h$). At higher flow rates, the performance of the collector/regenerator was clearly surpassed by that of the indirect solar regenerator with preheating of liquid desiccant (SWH+WS-HX+Reg).

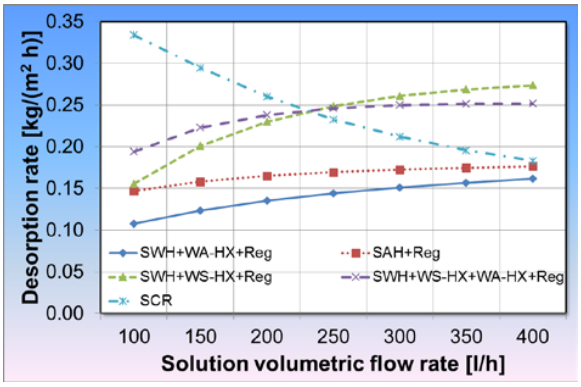

Fig. 9: Effect of the solution volumetric flow rate on the desorption rate of the solar regenerators with indirect and direct (pre)heating of the regenerating air and the desiccant solution.

5. Conclusions

The use of collector/regenerators contributes to reduce the installation costs and complexity of liquid desiccant systems by diminishing their number of components and by simplifying their control strategies. Moreover, the direct solar regenerator clearly outperforms the indirect ones at high absolute humidities, air volumetric flow rates higher than 300 m^3/h ($\dot{m}_a/\dot{m}_{s,in}$ = 1.187 with $\dot{V}_{s,in}=200\ l/h$), high inlet temperatures of air and solution as well as solution volumetric flow rates lower than 225 l/h ($\dot{m}_a/\dot{m}_{s,in}=1.282$ with $\dot{V}_a=300\ m^3/h$) while keeping constant the other operating parameters.

Acknowledgments

This work is sponsored by the Federal Ministry of Education and Research in framework of the program “Research at Universities of Applied Sciences – Funding stream Young Engineers” (contract number 03FH0041X4).

References

Duffie, J. A., Beckman, W. A., 2013. Radiation transmission through glazing: absorbed radiation, in: Solar engineering of thermal processes. John Wiley & Sons, Inc. pp. 202-214.

Gezahegn, H., Mullick, S. C., Jain, S., 2013. Optical and thermal performance of a liquid desiccant solar regenerator. Proc. of International Congress on Renewable Energy, KIIT University, Bhubaneswar, Odisha, 15-27.

Gnielinski, V., 2010. Fluid-particle heat transfer in flow through packed beds of solids, in: VDI Heat Atlas, V.-G.V.u. Chemieingenieurwesen, Springer, pp. 743-744.

Gnielinski, V., 1976. New equations for heat and mass transfer in turbulent pipe and channel flow. Int. Chem. Eng. 16(2), 359-367.

Gommed, K., Grossman, G., 2007. Experimental investigation of a liquid desiccant system for solar cooling and dehumidification. Sol. Energy 81(1), 131-138.

Grossman, G., Johannsen, A., 1981. Solar cooling and air conditioning. Prog. Energy Combust. Sci. 7(3), 185-228.

Guo, J., Lin, S., Bilbao, J. I., White, S. D., Sproul, A. B., 2017. A review of photovoltaic thermal (PV/T) heat utilisation with low temperature desiccant cooling and dehumidification. Renew. Sustain. Energy Rev. 67, 1-14.

Hawlader, M. N. A., Wood, B. D., Folkman, C. C., Stack, A. P., 1997. Solar assisted open-cycle absorption cooling: Performance of collector/regenerators. Int. J. Energ. Res. 21(6), 549-574.

Jamar, A., Majid, Z. A. A., Azmi, W. H., Norhafana, M., Razak, A. A., 2016. A review of water heating system for solar energy applications. Int. Commun. Heat Mass Transf. 76, 178-187.

Kabeel, A. E., 2005. Augmentation of the performance of solar regenerator of open absorption cooling system. Renew. Energ. 30(3), 327-338.

Kabeel, A. E., Hamed, M. H., Omara, Z. M., Kandeal, A. W., 2017. Solar air heaters: design configurations, improvement methods and applications - a detailed review. Renew. Sustain. Energy Rev. 70, 1189-1206.

Katejanekarn, T., Kumar, S., 2008. Performance of a solar-regenerated liquid desiccant ventilation pre-conditioning system. Energy Build. 40(7), 1252-1267.

Kaushik, S. C., Kaudinya, J. V., Yadav, Y. K., 1992. Studies on some solar collector/regenerator systems for open cycle absorption air conditioning/liquid desiccant cooling systems. Heat Recov. Syst. CHP 12(4), 357-363.

Martin, V., Goswami, Y., 2000. Effectiveness of heat and mass transfer processes in a packed bed liquid desiccant dehumidifier/regenerator. HVAC&R. Res. 6(1), 21-39.

Mercer, W. E., Pearce, W. M., Hitchcock, J. E., 1967. Laminar forced convection in the entrance region between parallel flat plates. J. Heat Transfer 89(3), 251-256.

Yang, R., Wang, P. L., 2001. A simulation study of performance evaluation of single-glazed and double-glazed collectors/regenerators for an open-cycle absorption solar cooling system. Sol. Energy 71(4), 263-268.